Beyond the AHA 17-Segment Model: Motion-Driven Parcellation of the Left Ventricle

Wenjia Bai[1(✉)], Devis Peressutti[2], Sarah Parisot[1], Ozan Oktay[1], Martin Rajchl[1], Declan O'Regan[3], Stuart Cook[3,4], Andrew King[2], and Daniel Rueckert[1]

[1] Biomedical Image Analysis Group, Department of Computing, Imperial College London, London, UK
w.bai@imperial.ac.uk
[2] Division of Imaging Sciences and Biomedical Engineering, King's College London, London, UK
[3] MRC Clinical Sciences Centre, Hammersmith Hospital, Imperial College London, London, UK
[4] Duke-NUS Graduate Medical School, Singapore, Singapore

Abstract. A major challenge for cardiac motion analysis is the high-dimensionality of the motion data. Conventionally, the AHA model is used for dimensionality reduction, which divides the left ventricle into 17 segments using criteria based on anatomical structures. In this paper, a novel method is proposed to divide the left ventricle into homogeneous parcels in terms of motion trajectories. We demonstrate that the motion-driven parcellation has good reproducibility and use it for data reduction and motion description on a dataset of 1093 subjects. The resulting motion descriptor achieves high performance on two exemplar applications, namely gender and age predictions. The proposed method has the potential to be applied to groupwise motion analysis.

1 Introduction

The evaluation of cardiac function involves assessing not only the anatomy of the heart but also its motion [1,2]. Modern imaging modalities such as magnetic resonance (MR) and ultrasound (US) provide a convenient way for visualisation and analysis of cardiac motion. A major challenge for cardiac motion analysis is the high-dimensionality of the image data, both spatially and temporally. In order to reduce the dimensionality, the 17-segment model proposed by the American Heart Association (AHA) is conventionally used to divide the image data into regional segments using criteria based on anatomical structures [3].

For cardiac motion analysis, however, it is possible that certain regions with unique motion signatures, e.g. regions with scars or other pathologies, may not align with the pre-defined anatomical segments of the AHA model. In this work, we propose to parcellate the left ventricle (LV) into a number of segments such that each segment contains similar and consistent motion information. To the

O. Camara et al. (Eds.): STACOM 2015, LNCS 9534, pp. 13–20, 2016.
DOI: 10.1007/978-3-319-28712-6_2

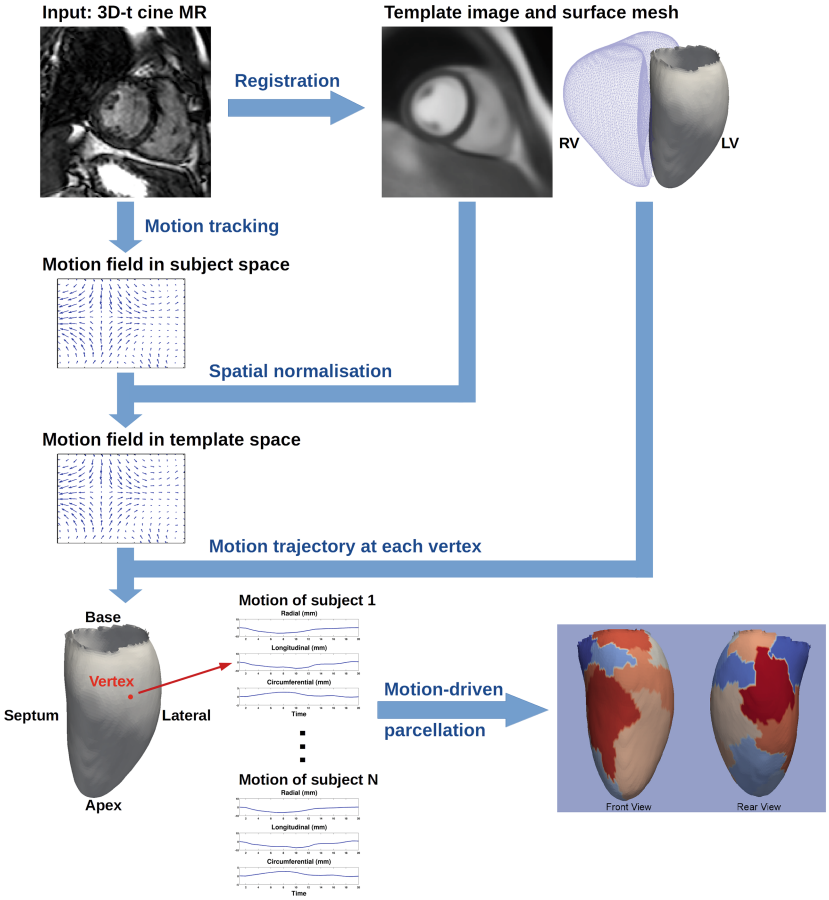

Fig. 1. The flowchart consists of motion tracking, spatial normalisation and motion-driven parcellation.

best of our knowledge, this is the first time that motion-driven parcellation is proposed for the heart, although a similar idea, functional parcellation, has become common for brain analysis [4]. Using a large dataset of cardiac MR images from 1093 subjects, we demonstrate that the parcellation has good reproducibility and can be used to reduce data dimensionality and be applied to cardiac motion analysis.

2 Methods

In this work, we are interested in the motion of the LV and parcellation is based on the motion tracking results for the LV. We employ a group-wise parcellation method, in which the motion fields of a large population are normalised onto a

template surface mesh and then clustering is applied to the normalised motion feature vectors of the vertices. Figure 1 illustrates the flowchart of the method and we will explain each step in the following.

2.1 Data Description

The dataset used in this work consists of cardiac MR images of 1093 normal subjects (493 males, 600 females; age range 19–75 yr, mean 40.1 yr). Cardiac MR was performed on a 1.5T Philips Achieva system (Best, Netherlands) using the 3D cine balanced steady-state free precession (b-SSFP) sequence. The voxel spacing is $1.25 \times 1.25 \times 2$ mm. Cine MR images are used here for cardiac motion analysis, which consists of 20 time frames across a cardiac cycle with the 0-th frame representing the end-diastolic (ED) frame. Other imaging modalities such as tagged MR or ultrasound may also be used, which can capture the motion of the heart at a different spatio-temporal resolution and with different quality.

2.2 Motion Tracking

Motion tracking is performed for each subject using a 4D spatio-temporal B-spline image registration method with a sparseness regularisation term [5]. The motion field estimate is represented in the subject space by a displacement vector at each voxel and at each time frame t, which measures the displacement from the 0-th frame to the t-th frame.

2.3 Spatial Normalisation

Parcellation is performed in a template image space, as shown at the top-right corner of Fig. 1. To represent the motion fields of all the subjects in the template space, the subject images are aligned to the template image by non-rigid B-spline image registration [6]. Using the transformation between the template space and subject space, the motion field of each subject is transported to the template space. Let $\mathbf{x}' = T(\mathbf{x})$ denote the transformation from template to subject, where $\mathbf{x}$ and $\mathbf{x}'$ are respectively the coordinates in the template space and in the subject space. By considering the spatial transformation as a change of coordinates [7], we have,

$$\mathbf{d}(\mathbf{x}, t) = \mathbf{J}_{T^{-1}}(\mathbf{x}') \cdot \mathbf{d}'(\mathbf{x}', t) \tag{1}$$

where $\mathbf{d}'$ denotes the displacement in the subject space, $\mathbf{d}$ denotes the corresponding displacement in the template space and $\mathbf{J}_{T^{-1}}(\mathbf{x}') \equiv \frac{d\mathbf{x}}{d\mathbf{x}'}$ denotes the Jacobian matrix of the inverse transformation.

2.4 Motion-Driven Parcellation

Let M denote the number of vertices on the template surface mesh (8528 vertices in our case), N denote the number of subjects and F denote the dimension of the motion trajectory. The motion trajectory at a vertex is defined as the

concatenation of the radial, longitudinal and circumferential displacements of all the time frames across the cardiac cycle. Then at each vertex, we concatenate the motion trajectory of all the subjects, resulting in a feature vector of dimension $n = NF$. Parcellation can be regarded as clustering of the M vertices into K groups such that the vertices in each group display similar group-wise motion trajectory. It produces a reduced representation of the input data.

A number of approaches have been proposed for clustering, such as K-means, Ward's algorithm [8], EM algorithm which models the clusters as a mixture of Gaussians or other distributions [9] and graph partitioning [10]. We use the Ward's algorithm which has been shown to perform with good reproducibility in [11].

Ward's algorithm starts by considering each vertex as a cluster [8]. Then at each step, it merges the two closest clusters. It defines the loss function as the within-cluster variance and the two clusters which lead to the minimal increase of the loss function are selected for merging,

$$(c_1, c_2) = \arg\min_{c_1,c_2} \sum_{i \in c_1 \cup c_2} ||\mathbf{y}_i - \bar{\mathbf{y}}_{c_1 \cup c_2}||^2 - \Big(\sum_{i \in c_1} ||\mathbf{y}_i - \bar{\mathbf{y}}_{c_1}||^2 + \sum_{i \in c_2} ||\mathbf{y}_i - \bar{\mathbf{y}}_{c_2}||^2 \Big) \tag{2}$$

where c_1 and c_2 denote the clusters to be merged, $\mathbf{y}_i$ denotes a data point in the cluster and $\bar{\mathbf{y}}$ denotes the cluster mean.

The feature vector at each vertex is of n dimension. To reduce the computational cost of clustering, we reduce the dimension of the feature vector using PCA. We keep the first few principal components which account for 95 % of the data variance and thus reduce the feature vector dimension to 36. Ward's clustering is applied to the data after dimensionality reduction.

2.5 Reproducibility Index

To evaluate the reproducibility of the clustering or the parcellation, we use the Rand index as in work [11], which measures the agreements between two clustering results [12]. For M vertices, the total number of vertex pairs is $\binom{M}{2}$. Let a denote the number of vertex pairs that are placed in the same class in clustering 1 and also in the same class in clustering 2, b denote the number of vertex pairs that are placed in different classes in clustering 1 and also in different classes in clustering 2. The Rand index is defined as $R = (a+b)/\binom{M}{2}$. It is a value between 0 and 1, with 0 indicating that two clusterings do not agree with each other at all and 1 indicating that two clusterings are the same.

3 Experiments and Results

3.1 Visualisation

We empirically set the number of clusters for Ward's clustering to 17 to be comparable with the AHA 17-segment model. Figure 2 compares the AHA 17-segment model with the 17-segment model produced by motion-driven parcellation, which we name as "functional 17-segment model" for short. The AHA

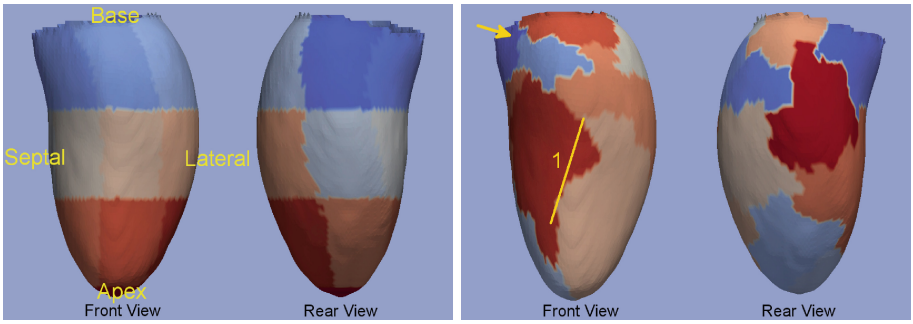

(a) AHA 17-segment model (b) Functional 17-segment model

Fig. 2. Comparison of the anatomical segment model with the functional segment model.

model, Fig. 2(a), distributes 35 % of the volume to the basal part (6 segments), 35 % to the mid-ventricular part (6 segments), 30 % to the apical part (4 segments) and 5 % to the apex [3]. The functional 17-segment model does not follow the empirical definition for the volume percentage, but instead it creates segments which have homogeneous motion trajectories. There are several interesting findings in the functionally parcellated model, as shown in Fig. 2(b). First, the segments are not of equal size. Those at the basal part (pointed by the arrow) are relatively small, which hints that the variance of motion is large at this part so the parcellation needs to be dense. Second, the septal wall (left of line 1) is separated from the other parts of the wall (right of line 1), which is physiologically reasonable, because the motion of the septal wall is restricted by its connection with the right ventricle while the other parts are more free.

3.2 Reproducibility

We evaluate the reproducibility of the parcellation by comparing the clustering results on two subsets. We randomly select 500 subjects as the first set and 500 subjects as the second set and the two sets are mutually exclusive. Motion-driven parcellation is performed on both sets and the clustering results are compared visually and quantitatively. As Fig. 3 shows, the septal wall (left of line 1) is consistently separated from the lateral wall (right of line 1) on both subsets. The basal part (above line 2) is consistently separated from the mid-ventricular part (below line 2). The separations at line 3 and line 4 are also consistent. These separating lines and regions are also noticeable on the parcellation based on the full dataset, Fig. 2(b).

To quantitatively evaluate the reproducibility of parcellation, we repeat the random subset division for 10 times and measure the Rand index between the two parcellations. The mean Rand index is 0.922 ± 0.006. This means that for 92.2 % of the vertex pairs, the two parcellations agree on whether or not they belong to the same parcel.

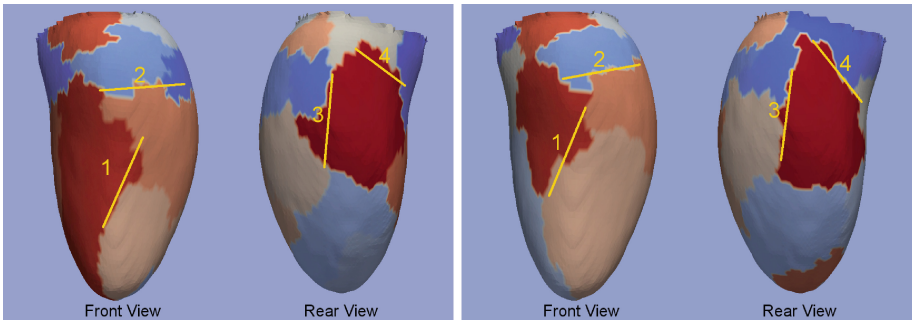

(a) Subset 1 (b) Subset 2

Fig. 3. The parcellation results based on two mutually exclusive subsets, each containing 500 subjects. The colour codes of the two parcellations are not exactly the same, because the cluster IDs given by the Ward's algorithm can be different in two runs. Please refer to the paragraph for the explanation of the lines (Color figure online).

Table 1. Gender and age prediction performance using the motion descriptors with different number of parcels and with the AHA 17-segment model.

	Gender Accuracy	Age Correlation
7 parcels	87.4 %	0.823
17 parcels	88.0 %	0.830
27 parcels	**89.0 %**	0.831
37 parcels	88.6 %	**0.834**
AHA	88.9 %	0.827

3.3 Application: Classification

Parcellation is often used for dimensionality reduction and it has a wide range of potential applications. In this study, we use it to extract a motion descriptor for cardiac motion analysis. We compute the mean motion trajectory for each parcel and concatenate them to form a motion descriptor of the left ventricle. We demonstrate the ability of the motion descriptor using two exemplar classification tasks, gender classification and age prediction. For comparison, we test the performance when different numbers of clusters are used in parcellation and when the AHA 17-segment model is used for computing the motion descriptor.

We performed 10-fold cross-validation on the set of 1093 subjects. Given the motion descriptor as input, SVM classifiers with RBF kernels were trained on the training set and then applied to the testing set to predict the gender and age of a given subject. The prediction accuracy for gender and the correlation coefficient between predicted age and real age are evaluated. The results are reported in Table 1 and plotted in Fig. 4. It shows that using the parcellation-based motion descriptor, we can achieve high accuracy for both gender and age prediction. For gender prediction, motion-driven parcellation using 27 segments

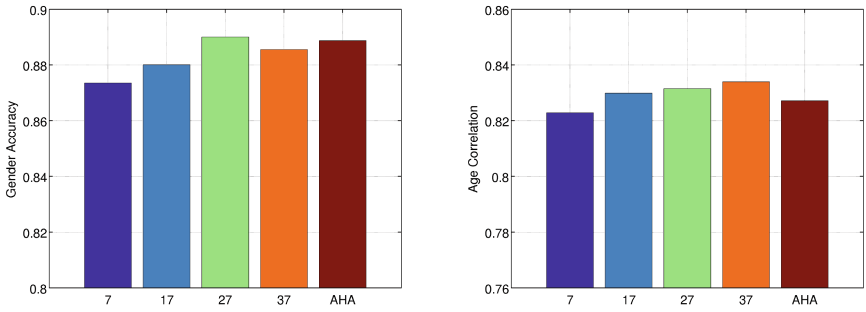

(a) Gender prediction (b) Age prediction

Fig. 4. Gender and age prediction performance using the motion descriptors with different number of parcels (7, 17, 27 or 37 parcels) and with the AHA 17-segment model.

achieves slightly better performance than the AHA model ($p > 0.01$). For age prediction, motion-driven parcellation using 17, 27 or 37 parcels perform better than the AHA model ($p < 0.01$). In addition, using a small number of parcels such as 7 only slightly sacrifices the performance. The reason is that gender and age affects the cardiac motion globally and therefore a small number of parcels can also encode the information.

4 Conclusions

To conclude, a novel method is proposed for cardiac motion analysis, which parcellates the left ventricle based on motion information instead of using pre-defined anatomical structure. Although each individual component of the method (registration, transport and clustering) may not be novel in itself, they are combined to form a novel way to investigate cardiac motion. It can be used for visualising regional clustering of motion and for reducing high-dimensional motion data. As an exploratory step in this direction, we use the displacement trajectory to represent cardiac motion, but other representation such as velocity, strain or electroanatomical recording can be explored in future in this framework.

In the work, our data are all healthy subjects and therefore we only demonstrate the motion descriptor on two exemplar classifications, gender and age predictions. These two factors affect motion globally and may not be the best examples for demonstrating a regional descriptor. However, the proposed method has the potential to be extended to other applications, where regional descriptors are more important. For example, it can be used for groupwise motion analysis in which two groups of subjects present different local motion patterns.

A limitation of the proposed method is that it may be more suited to group analysis instead of case studies. A direction of future work is to include patients data with similar pathologies into our dataset and to perform motion analysis and comparison between the healthy and the patients.

References

1. Mor-Avi, V., Lang, R.M., Badano, L.P., Belohlavek, M., et al.: Current and evolving echocardiographic techniques for the quantitative evaluation of cardiac mechanics. Eur. J. Echocardiogr. **12**(3), 167–205 (2011)
2. Suinesiaputra, A., Frangi, A.F., Kaandorp, T., Lamb, H.J., Bax, J.J., Reiber, J., Lelieveldt, B.P.F.: Automated detection of regional wall motion abnormalities based on a statistical model applied to multislice short-axis cardiac MR images. IEEE Trans. Med. Imaging **28**(4), 595–607 (2009)
3. Cerqueira, M.D., Weissman, N.J., Dilsizian, V., Jacobs, A.K., et al.: Standardized myocardial segmentation and nomenclature for tomographic imaging of the heart. Circulation **105**(4), 539–542 (2002)
4. Yeo, B.T.T., Krienen, F.M., Sepulcre, J., Sabuncu, M.R., Lashkari, D., et al.: The organization of the human cerebral cortex estimated by intrinsic functional connectivity. J. Neurophysiol. **106**(3), 1125–1165 (2011)
5. Shi, W., Jantsch, M., Aljabar, P., Pizarro, L., Bai, W., Wang, H., O'Regan, D., Zhuang, X., Rueckert, D.: Temporal sparse free-form deformations. Med. Image Anal. **17**(7), 779–789 (2013)
6. Rueckert, D., Sonoda, L.I., Hayes, C., Hill, D.L.G., Leach, M.O., Hawkes, D.J.: Nonrigid registration using free-form deformations: application to breast MR images. IEEE Trans. Med. Imag. **18**(8), 712–721 (1999)
7. Duchateau, N., De Craene, M., Piella, G., Silva, E., Doltra, A., Sitges, M., Bijnens, B.H., Frangi, A.F.: A spatiotemporal statistical atlas of motion for the quantification of abnormal myocardial tissue velocities. Med. Image Anal. **15**(3), 316–328 (2011)
8. Ward, J.H.: Hierarchical grouping to optimize an objective function. J. Am. Stat. Assoc. **58**(301), 236–244 (1963)
9. Kulis, B., Jordan, M.I.: Revisiting k-means: New algorithms via Bayesian nonparametrics. In: ICML, pp. 513–520 (2012)
10. Shi, J., Malik, J.: Normalized cuts and image segmentation. IEEE Trans. Pattern Anal. Mach. Intell. **22**(8), 888–905 (2000)
11. Thirion, B., Varoquaux, G., Dohmatob, E., Poline, J.B.: Which fMRI clustering gives good brain parcellations? Front. Neurosci. **8**, 13 (2014)
12. Hubert, L., Arabie, P.: Comparing partitions. J. Classif. **2**(1), 193–218 (1985)

http://www.springer.com/978-3-319-28711-9

Statistical Atlases and Computational Models of the Heart. Imaging and Modelling Challenges
6th International Workshop, STACOM 2015, Held in Conjunction with MICCAI 2015, Munich, Germany, October 9, 2015, Revised Selected Papers
Camara, O.; Mansi, T.; Pop, M.; Rhode, K.; Sermesant, M.; Young, A. (Eds.)
2016, XI, 218 p. 91 illus., Softcover
ISBN: 978-3-319-28711-9